

A LARGE BUBBLE AROUND THE CRAB NEBULA

ROGER W. ROMANI, WILLIAM T. REACH, BON CHUL KOO, AND CARL HEILES

Department of Astronomy, University of California, Berkeley

Received 1989 August 8; accepted 1989 November 1

ABSTRACT

IRAS and 21 cm observations of the interstellar medium around the Crab nebula show evidence of a large bubble surrounded by a partial shell. If located at the canonical 2 kpc distance of the Crab pulsar, the shell is estimated to have a radius of ~ 90 pc and to contain $\sim 5 \times 10^4 M_\odot$ of swept-up gas. We discuss how interior conditions of this bubble can have important implications for observations of the Crab and describe how presupernova evolution of the pulsar progenitor has affected its local environment.

Subject headings: pulsars — stars: individual (PSR 0523 + 21) — stars: supernovae — stars: winds

I. INTRODUCTION

The Crab nebula and its pulsar, remnants of the historical supernova of AD 1054, are among the most thoroughly studied astrophysical objects. This scrutiny has highlighted a number of peculiarities: the remnant is helium rich, has an unusually low expansion velocity, and is dynamically dominated by the power input of the central pulsar. This pulsar-powered synchrotron nebula has become the archetype for the “plerionic” or center-filled supernova remnants. However, despite several careful searches, a classical shell-like remnant surrounding this central plerion has not been found (e.g., Fesen and Ketelsen 1985; Velusamy 1985; Schattenburg *et al.* 1980). In one scenario that explains the lack of an observed shell, the pre-supernova star lost virtually all of its hydrogen envelope before the explosion, leaving little mass in the blast wave to form a fast shell-like shock. Alternatively, if the circumstellar environment is suitably modified, a fast shell of hydrogen may be present but as yet only small amounts of surrounding material are swept up and shocked, keeping the shell well below present observational limits.

As discussed by Chevalier (1985), the circumstellar environment of the pre-supernova star can dramatically affect the appearance of the supernova remnant. This environment is modified as a consequence of ionization from the progenitor star, mass loss in stellar winds, and the energy input by other nearby sources. We have examined large-scale survey data for evidence of such processes, which may help describe the evolution of the Crab progenitor as well as explicate peculiarities of the present remnant.

II. OBSERVATIONS

Examination of the *IRAS* skyflux maps shows a large deficit surrounding the Crab nebula which is bounded by excess emission forming a partial shell. In Figure 1 (Plate L6) we show a mosaic of the $100 \mu\text{m}$ flux from four skyflux fields. The Crab nebula itself is visible as a bright point-like source at $05^{\text{h}}31^{\text{m}}31^{\text{s}}$, $+21^\circ58'54''$ (1950). The boundary is prominent along the Galactic plane (visible in the image to the northeast) and seems to extend further from the Crab to the south, becoming faint to the southeast. An approximate center for the resulting bubble is at $5^{\text{h}}29^{\text{m}}$, $+21^\circ46'$ with an angular radius of ~ 2.5 . Summing over an annulus from 2° to 3° and subtracting the local background, we can estimate the total $100 \mu\text{m}$ flux as 2.3×10^4 Jy. The structure is also prominent at $60 \mu\text{m}$ with a

flux of ~ 3700 Jy and is visible in the short-wavelength bands, as well; at $12 \mu\text{m}$ the maps indicate ~ 1500 Jy. Systematic errors in estimating the boundaries and background should make these fluxes uncertain by $\sim 30\%$. The Galactic anticenter is a complex region with a number of partial shells; however the strong deficit in the roughly circular interior and the enhanced emission at the bubble's edge suggest a coherent structure.

From the $60 \mu\text{m}/100 \mu\text{m}$ flux ratio and a $\lambda^{-1.5}$ emissivity law we can estimate the temperature of the dust shell as $\sim 23 \pm 2$ K. This temperature is only slightly larger than the mean interstellar value ~ 20 K and substantially cooler than the 30–50 K estimated for many supernova remnants (Arendt 1989), indicating that the dust is not strongly heated by shocks or embedded sources. For our estimated temperature and normal gas to dust ratios, we can relate the *IRAS* flux density to the gas column density by $1 \text{ MJy sr}^{-1} (100 \mu\text{m}) \sim 8.5 \times 10^{19} \text{ cm}^{-2} (N_{\text{H}})$ (Boulanger and Perault 1988). Unlike the presumably shock-warmed, relatively young supernova remnant shells seen by Shull, Fesen, and Saken (1989), this structure is not prominent in $60 \mu\text{m}/100 \mu\text{m}$ flux ratio maps.

The Crab nebula is assumed to lie at $2.0d_2$ kpc, as estimated from kinematic studies of the nebular filaments (Trimble 1971). The observed infrared luminosity is accordingly $\sim 3 \times 10^4 d_2^2 L_\odot$. The total shell mass may be empirically estimated from the $100 \mu\text{m}$ flux, using the conversion factor above, as $\sim 6 \times 10^4 d_2^2 M_\odot$. Alternatively, from the $T_d(60 \mu\text{m}/100 \mu\text{m})$ dust temperature and the observed flux, the total dust mass is

$$M_d = \frac{\pi D^2 S_\nu}{B_\nu(T_d) \kappa_\nu} \sim 3 \times 10^{-5} [e^{(1.44K/T_d)} - 1] d_2^2 S_{100 \mu\text{m}} (\text{Jy}) M_\odot \quad (1)$$

where B_ν and S_ν are the Planck function and the spectral density and κ_ν , the grain emissivity, is $\sim 50 \text{ cm}^2 \text{ g}$ at $100 \mu\text{m}$ (e.g., Draine and Lee 1984). This gives a dust mass $\sim 350 d_2^2 M_\odot$ which for a dust-to-gas mass ratio $z_d = 0.0075$ corresponds to a total shell mass of $\sim 4.7 \times 10^4 d_2^2 M_\odot$. The strong temperature dependence in equation (1) makes these estimates uncertain by factors of a few. If the observed shell of radius $87 d_2$ pc represents mass swept up from the shell interior, the mean total density in the volume evacuated was $\sim 0.7 d_2^{-1} \text{ cm}^{-3}$.

We have also found evidence for the cold gas associated with the *IRAS* shell in the H I survey data of Weaver and Williams

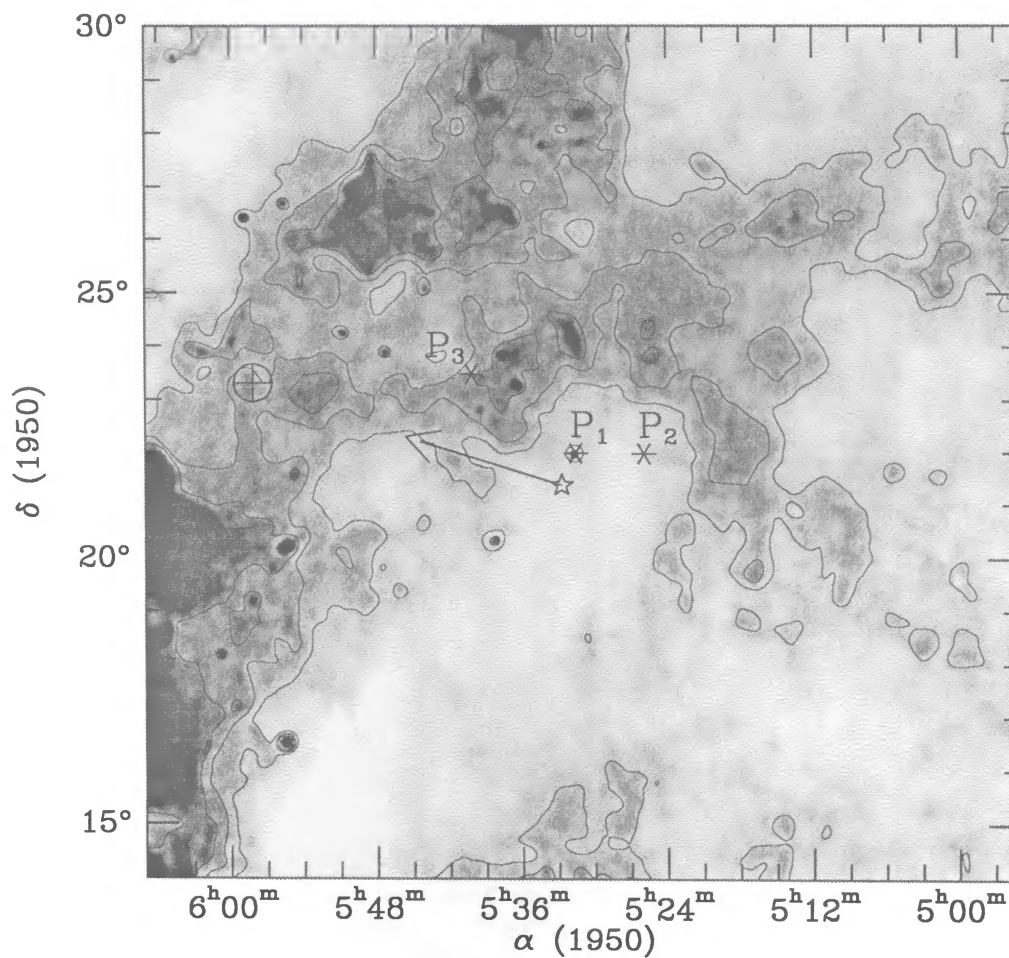


FIG. 1.—*IRAS* 100 μm emission in the vicinity of the Crab nebula. Contour levels are 35, 40, and 45 MJy sr^{-1} . Asterisks (*) indicate the positions of three young pulsars (Crab = PRS 0531 = P1, PRS 0525 = P2, PSR 05440 = P3), the O7.5 star HD 36879 (star) and the galactic cluster NGC 2129 (circled cross) are also shown. The proper motion over 10^6 yr for HD 36879 is indicated by the solid line: $\mu_\alpha = -11 \pm 8 \times 10^{-3}$ arcsec yr^{-1} , $\mu_\delta = -3 \pm 8 \times 10^{-3}$ arcsec yr^{-1} (nominal uncertainties).

ROMANI, HEILES, KOO, AND REACH (see 349, L51)

(1974). In Figure 2 (Plate L7) we show a half-tone and contour map of the H I emission in the velocity range -11.1 to -9.0 km s^{-1} . There is substantial emission in a ridge crossing the position of the Crab. In addition, there is a large complex of emission to the north with high column densities at velocities near the LSR. The southern arm of the shell is prominent below the Crab, and, while the ridge of the shell is not well defined to the north, the H I column shows substantial correlation with the *IRAS* dust emission. The shell is visible in neutral hydrogen at LSR velocities from -17 to -3 km s^{-1} . There is no evidence for expansion over this velocity range. It thus appears that the shell has merged with the general ISM, and its velocity structure is dominated by random cloud motions at the local sound speed.

In the 2° - 3° annulus the excess antenna temperature times line width is ~ 93 K km s^{-1} . The dense cloud to the northwest contributes strongly to the background in the annulus, so we sum over the other three quadrants and renormalize to the total area. Using the conversion factor $N_{\text{H}} = 1.8 \times 10^{18} [\Delta T(\text{K}) \Delta v(\text{km s}^{-1})] \text{ cm}^{-2}$ and a distance of 2 kpc, this gives an estimated mass in the annulus of $\sim 2 \times 10^4 d_2^2 M_\odot$. This is in reasonable agreement with the masses inferred from the dust emission, suggesting gas-to-dust ratios greater than or approximately normal and little destruction of grains in the shell formation process. Dense condensations in the shell may well contain molecular gas, in which case the total gas mass is underestimated. The ridge of H I crossing the position of the Crab has a comparable amount of gas and while not prominent in the infrared, may also represent part of the shell.

Spectra of H I in absorption against the bright continuum of the Crab nebula shows evidence of the shell gas, as well. In high signal-to-noise observations taken at Hat Creek, strong H I emission is seen at roughly -10 , $+2$, and $+10$ km s^{-1} (LSR) at the position of the Crab, with weaker components extending from about -50 to about $+30$ km s^{-1} . Differencing with adjacent pointings, the spectrum obtained shows absorption with $\tau \sim 1$ at roughly $+3$ km s^{-1} and roughly $+12$ km s^{-1} ; interferometric studies with higher velocity resolution (Greisen 1973) have shown this gas to have substantial velocity structure as well as significant variation in absorption optical depth across the face of the Crab nebula. We also find $\tau \sim 0.3$ absorption at roughly -10 km s^{-1} , indicating that gas from the bright ridge at $b \sim -6^\circ$ and/or the shell has strong spatial variations or lies predominantly in front of the Crab nebula. Significant absorption is also seen out to roughly -50 km s^{-1} .

Finally, examining the large-scale H α plates of Sivan (1974), we find a bright, unresolved source at the position of the Crab, surrounded by a "halo" of radius $\sim 2^\circ$ in which the emission appears slightly depressed below the local background. This survey apparently reveals structures down to an emission measure less than ~ 30 cm^{-6} pc; if the mean density of the ionized gas into which the bubble expands is ~ 0.7 cm^{-3} , then the volume cleared by the bubble's formation will cause an emission-measure deficit of this order.

III. DISCUSSION AND CONCLUSIONS

We propose that the bubble is a fossil created by the ionizing flux and stellar winds of several early-type stars, a few of which have left remnants in the region. The Crab progenitor will have contributed, but, as argued below, probably did not dominate generation of the present bubble. Large variations in external density and pressure at this distance below the plane, as well as a distributed energy input from several stellar sources can

explain the bubble's irregular morphology and apparent "blow out" away from the Galactic disk.

In Figure 1, we show the positions of several massive stars or their evolutionary products. In addition to the Crab itself (age $\sim 10^3$ yr), the pulsar PSR 0525+21 (age $\sim 10^6$ yr) is superposed within the bubble and, having a dispersion measure similar to the Crab, apparently lies at a comparable distance. Observations of interstellar scintillations from this source suggest a transverse speed of ~ 100 km s^{-1} (Cordes 1986); proper-motion measurements (Lyne, Anderson, and Salter 1982) unfortunately only bound the (two-dimensional) space velocity to be less than ~ 300 km s^{-1} . It is therefore unclear if this pulsar's progenitor was within the present confines of the bubble before the supernova event. A third young pulsar in the vicinity, PSR 0540+23 (age $\sim 3 \times 10^5$ yr), is also indicated. This pulsar has a dispersion measure larger than those of the Crab and PSR 0525 by $\delta\text{DM} \sim 20$ cm^{-3} pc; accordingly, it is usually assigned a distance of ~ 2.6 kpc. However, we note that if the mean ionized density in the vicinity of the bubble is ~ 0.2 cm^{-3} (making this part of the warm, ionized interstellar medium; Kulkarni and Heiles 1988) then the ~ 100 pc path through the lower density medium of the hot bubble interior will decrease the DM of the Crab and its companion by an amount comparable to the discrepancy above. Thus all three pulsars may lie at a similar distance. PSR 0540+23 has a scintillation determined velocity of ~ 160 km s^{-1} , and if it has traveled from the Galactic plane it will not have yet interacted with the bubble interior. However, this object's progenitor might well have been born in the same burst of star formation that formed the other early-type stars in this region.

From catalogs of Galactic O stars we have found one object superposed within the *IRAS* bubble. This is HD 36879 = SAO 77293, estimated in the catalog of Gruz-González *et al.* (1974) to be of spectral type O7.5 III and to lie at a distance of 1.94 kpc. This distance would place the star in the bubble interior; there is possible morphological support for this association in that there is a "trail" of decreased *IRAS* emission to the northeast of the O star (Fig. 1). The position angle agrees with that of the nominal, but very low significance, proper motion. Interestingly, this vector leads back to the galactic cluster NGC 2129, which at 2.1 kpc distance presently contains stellar types as early as B1. The proper-motion limits on HD 36879 are sufficient to allow travel from this birth site in its $\sim 10^7$ yr main-sequence lifetime. The nebular proper motion (which presumably reflects that of the Crab progenitor) is estimated by Trimble (1971) as ($\mu_\alpha = 0.0 \pm 0.7 \times 10^{-4}$ arcsec yr $^{-1}$, $\mu_\delta = -1.6 \pm 0.7 \times 10^{-4}$ arcsec yr $^{-1}$), which corresponds to a relatively small space velocity ~ 15 km s^{-1} from the north. This suggests that the Crab would not share parentage with HD 36879. However, we note that stars of discrepant age might still be born in the same cluster if the massive star formation proceeds in several bursts or is asynchronous on times scales of $\sim 10^7$ yr.

We posit that several times 10^7 yr ago the Crab progenitor entered a low-density portion of the ISM, which was heated and cleared of clouds by the ionizing luminosity, stellar winds, and supernova blast waves of a group of early-type stars, perhaps including the progenitor of PSR 0540. A few million years ago HD 36879 moved into this region, and with its estimated ionizing flux $S \sim 10^{49}$ s $^{-1}$, began to evaporate the bay to the southeast of the Crab. This flux should drive an *R* front into the surrounding gas, growing toward the Strömgren

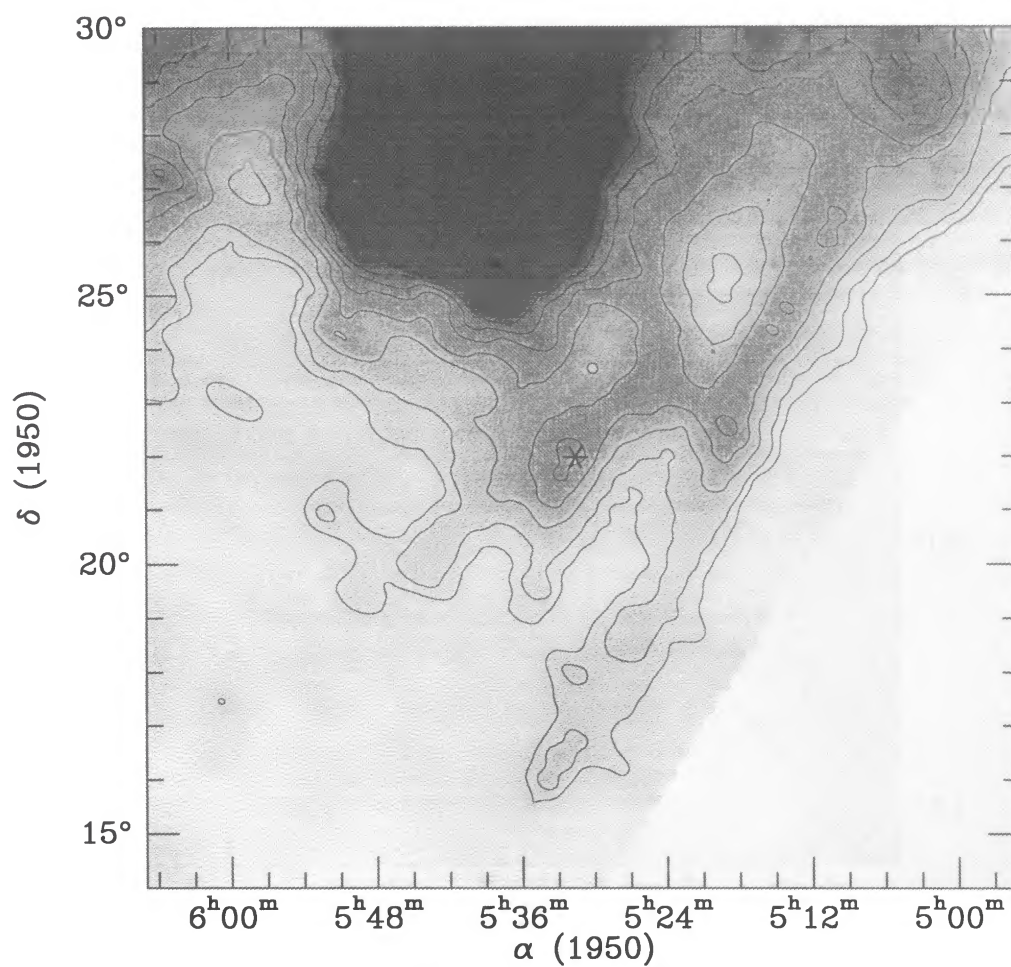


FIG. 2.—Contour and half-tone map of H I emission near the Crab nebula in the velocity range -11 to -9 km s^{-1} . Contours are at $35, 40, 50, 60, \dots \text{ K km s}^{-1}$ and the Crab is indicated by an asterisk (*). The blank area to the southwest represents the $b = -10^\circ$ limit of the Weaver-Williams survey.

ROMANI, HEILES, KOO, AND REACH (see 349, L52)

radius of $\sim 64n^{-2/3}$ pc at $\sim S/(4\pi r^2 n) \gtrsim 200n^{-1/3}$ km s $^{-1}$. The absence of any bounding H II region for more than $\sim 1^\circ$ around the star already limits the density within the bubble to less than ~ 2.5 cm $^{-3}$; the true density is probably much lower.

From nuclear abundances in the Crab nebula filaments Nomoto (1985) has estimated the mass of the Crab progenitor to be $8 M_\odot \lesssim M \lesssim 13 M_\odot$, which corresponds to main-sequence spectral type in the range $\sim O9.5$ – $B1.5$. The lifetimes of such stars are ~ 1.8 – 4.5×10^7 yr (Maeder and Maynet 1988). For illustrative purposes we consider a $9 M_\odot$ star, updating the values of Chevalier (1985). Maeder (1981) indicates that during the main-sequence lifetime of 2.4×10^7 yr the star has a fast $\sim 0.7 \times 10^3$ km s $^{-1}$ “blue” wind of strength $\sim 2 \times 10^{-8} M_\odot$ yr $^{-1}$, although these values are quite uncertain.

As noted by Chevalier (1985), the blue wind will shock at $\sim 2.3(\dot{M}_{-8} v_3/P_{-13})^{1/2}$ pc for a bubble pressure of 10^{-13} g cm $^{-1}$ s $^{-2}$, with postshock ionized gas at $T_b = 3\mu_b v_w^2/16k \sim 1.4 \times 10^7 v_3^2$ K which gives $\sim 7 \times 10^6$ K for our fiducial “blue” wind parameters. This hot shocked wind blows a cavity into the surrounding medium of the large-scale bubble. As this cavity grows it sweeps up the external mass in a shell of radius

$$r \sim 40 \left(\frac{\dot{M}_{-8} v_3^2}{n_0} \right)^{1/5} t_7^{3/5} \text{ pc}, \quad (2)$$

slowing until the ram pressure of the external medium is comparable to the static pressure; at this point the expanding cavity becomes transonic. This radius is

$$r_s \sim 37(\dot{M}_{-8} v_3^2)^{1/2} n_0^{1/4} P_{-13}^{-3/4} \text{ pc}, \quad (3)$$

which is reached in $\sim 9 \times 10^6 (\dot{M}_{-8} v_3^2)^{1/2} n_0^{3/4} P_{-13}^{-5/4}$ yr. At a bubble pressure 2000 K cm $^{-3}$ and an external density of ~ 0.7 cm $^{-3}$ the cavity reaches ~ 16 pc; thereafter the surrounding gas can begin to finger into the hot medium of the cavity interior, and there is no longer a clear division between the swept-up gas and the shocked blue wind. This mixing can substantially increase the density of the hot cavity gas. The subsequent fate of the blue wind cavity then depends on the cooling time of the mixed surface. Taking the cooling time to be $\tau_c \sim 500 P_{-13} \Lambda_{-23}^{-1} n^{-2}$ yr, with $\Lambda/10^{-23}$ ergs cm $^{-3}$ s $^{-1} = \Lambda_{-23} \sim 1$ for $T \gtrsim 10^5$ K, we see that the mixed gas will cool if $n_0 \gtrsim 0.02 P_{-13}^{9/11} (\Lambda_{-23}^2 \dot{M}_{-8} v_3^2)^{-2/11}$ cm $^{-3}$. Thus, unless the external medium is of quite low density, the wind cavity will stall at small radius and thereafter radiate away most of the wind luminosity.

If, however, the flow remains adiabatic, the shocked blue wind will continue to expand, doing work against the external medium. This will result in a cavity of size

$$r \sim 43 \left(\frac{\dot{M}_{-8} v_3^2}{P_{-13}} \right)^{1/3} t_7^{1/3} \text{ pc} \quad (4)$$

or ~ 45 pc with our fiducial values for the blue stellar wind. We note that unless the wind is substantially more energetic than our nominal values it will not be able to reach the observed ~ 90 pc radius of the bubble as a whole.

Stellar evolution calculations indicate that these intermediate-mass stars will, after leaving the main sequence, lose appreciable amounts of mass in a slow “red” phase wind. Suggested values for a $9 M_\odot$ star are a mean mass loss of $\dot{M} \sim 0.6 \times 10^{-6} M_\odot$ yr $^{-1}$ at a velocity $v_w \sim 10$ km s $^{-1}$ which lasts for $\sim 3.5 \times 10^6$ yr but increases substantially toward the end of the red phase (Maeder 1981). This wind expands into the

hot cavity containing the shocked “blue” wind and itself shocks at a radius

$$r_r = 2.3(\dot{M}_{-6} v_1/P_{-13})^{1/2} \text{ pc}. \quad (5)$$

The resulting temperature is 1.5×10^3 K and, given a cooling function of $\Lambda_{-23} \sim 0.01$ and a postshock density jump of ~ 4 , we estimate a cooling time of $\sim 10^6 v_1^2/(\Lambda_{-23} P_{-13})$ yr so that the shocked red wind can pile up at the interface. This will be dragged out by the progenitor velocity in a trail of length $\sim 15(v_w/15 \text{ km s}^{-1})\tau_6$ pc where the dense wind phase lasts $10^6 \tau_6$ yr. Blandford *et al.* (1983) have suggested that the trail corresponds to the Crab nebula’s observed “jet” of width ~ 0.5 pc and length ~ 1 pc. The northern location of this feature is in agreement with the rough proper motion of the nebula. However, kinematic and spectroscopic data (see Shull *et al.* 1985) demonstrate that the line-emitting filaments in the jet are more likely associated with the nebular gas. Nevertheless, we note that at the trail left by the red wind the confining magnetic pressure may be substantially reduced, providing a preferred location and channel for such an extrusion from the nebula. Examining the *IRAS* contour maps formed by two-dimensional high-resolution co-adds (Arendt 1989), we note an extension of the point source in a $\sim 15'$ trail to the north. This ~ 9 pc extension is of marginal significance and a $12 \mu\text{m}$ point source (IRAS 05316 + 2208) along this position angle may contribute much of the flux, but rough estimates indicate ~ 2 Jy in $100 \mu\text{m}$ flux and a $60 \mu\text{m}/100 \mu\text{m}$ flux ratio corresponding to a dust temperature of ~ 26 K. This gives a dust mass of $\sim 0.015 M_\odot$ and a total gas mass $\sim 2z_{0.0075}^{-1} M_\odot$. We note that high-resolution Arecibo observations should easily confirm the existence of this red wind or place limits on the fraction of the associated gas remaining neutral.

To assess the visibility of any “fast” ejecta from the remnant of the Crab’s H-rich envelope, it is important to determine the parameters of the circumstellar medium which it presently encounters. For a uniform density external medium, a presupernova envelope of mass $M_{ej} M_\odot$ and density profile $\sim r^{-7}$, and an explosion energy of $10^{51} E_{51}$ ergs, Chevalier (1982) shows that the outer fast shock will form at

$$R_{\text{out}} = 5.54 \left(\frac{E_{51}^2}{M_{ej} n_c} \right)^{1/7} t_3^{4/7} \text{ pc} \quad (6)$$

after $10^3 t_3$ yr. For $n_c \sim 3 \times 10^{-4}$ cm $^{-3}$, as in the shocked wind cavity, $5 M_\odot$ of ejecta would shock at ~ 15 pc; the amount of swept-up cavity gas is $\sim 0.1 M_\odot$. Observational evidence limits the amount of X-ray-emitting thermal gas swept up by a fast shock around the Crab to $\sim 1 M_\odot$ or less (Schattenburg *et al.* 1980). There are also strong limits on the radio synchrotron luminosity of a fast shell (Velusamy 1985), but conversion of these values to limits on the shocked mass are problematic. Thus, as long as the shell remains within the cavity evacuated by the shocked blue wind, it is likely to be fainter than present observational limits.

The extent of the blue wind cavity depends on the interior properties of our large-scale bubble. Thus, from equation (3), we see that if the bubble’s interior density is greater than ~ 1 cm $^{-3}$, the cavity will have a sonic radius larger than that of the present extent of the fast shock, and the gas shocked by the supernova blast wave would not yet be visible. For bubble interior densities $0.01 \text{ cm}^{-3} \lesssim n \lesssim 1 \text{ cm}^{-3}$, the cooling surface of the blue wind cavity will have been reached by the hydrogen envelope blast wave, which should then rapidly sweep up suffi-

cient mass from the bubble interior to provide detectable X-rays and convert the remnant evolution to the Sedov phase. Finally, for very low density, hot bubble interiors, the blue wind cavity will rapidly go sonic, but continue to expand according to equation (4), ensuring again that the fast shock will remain invisible in a low-density medium.

Future observations of the near-Crab environment, particularly more refined limits on thermal X-ray-emitting gas obtainable with AXAF, will help explicate the mystery of the Crab's missing blastwave shell. Neutral hydrogen emission and far-infrared studies of this area for evidence of the red wind trail will further bound the mass retained for the fast shock and should improve our understanding of the progenitor. In this *Letter*, we have described a large-scale bubble in the direction of the Crab. We argue that the Crab lies within this region which is evidence for large energy injection by its progenitor

and other recent massive star activity. In turn, we have shown how conditions within the bubble determine the extent of the circumstellar cavity cleared by the progenitor's "blue" wind. If sufficiently large, this cavity can explain the absence of an observed classical supernova blastwave. Thus the large-scale bubble in the interstellar medium provides an important vehicle for interpreting this well-studied, but as yet poorly understood, supernova remnant.

We wish to thank F. Bertoldi, D. Helfand, and C. McKee for numerous helpful discussions and the referee for a careful reading and helpful comments. W. T. R. thanks L. Dones for assistance in obtaining the *IRAS* data from NASA Ames Research Center. Support for this work was provided by NSF grants AST 86-15816 and 88-18544 and JPL contract 957286 as a subcontract under grant NAS 7918.

REFERENCES

- Arendt, R. G. 1989, *Ap. J. Suppl.*, **70**, 181.
 Blandford, R. D., Kennel, C. F., McKee, C. F., and Ostriker, J. P. 1983, *Nature*, **301**, 586.
 Boulanger, F., and Perault, M. 1988, *Ap. J.*, **330**, 964.
 Chevalier, R. 1982, *Ap. J.*, **258**, 790.
 ———. 1985, in *The Crab and Related Supernova Remnants*, ed. M. C. Kafatos and R. Henry (New York: Cambridge University Press), p. 63.
 Cordes, J. M. 1986, *Ap. J.*, **311**, 183.
 Cruz-González, C., Recillas-Cruz, E., Costero, R., Peimbert, M., and Torres-Peimbert, S. 1974, *Rev. Mexicana Astr. Af.*, **1**, 211.
 Draine, B. T., and Lee, H. M. 1984, *Ap. J.*, **285**, 89.
 Fesen, R. A., and Ketelsen, D. A. 1985, in *The Crab and Related Supernova Remnants*, ed. M. C. Kafatos and R. Henry (New York: Cambridge University Press), p. 89.
 Greisen, E. W. 1973, *Ap. J.*, **184**, 379.
 Kulkarni, S., and Heiles, C. 1987, in *Physical Processes in Interstellar Clouds*, ed. G. Morfill and M. Scholer (Dordrecht: Reidel), p. 13.
 Lyne, A. G., Anderson, B., and Salter, M. J. 1982, *M.N.R.A.S.*, **201**, 503.
 Maeder, A. 1981, *Astr. Ap.*, **102**, 401.
 Maeder, A., and Meynet, G. 1988, *Astr. Ap. Suppl.*, **76**, 411.
 Nomoto, K. 1985, in *The Crab and Related Supernova Remnants*, M. C. Kafatos and R. Henry (New York: Cambridge University Press), p. 97.
 Schattenburg, M. L., Canizares, C. R., Berg, C. J., Clark, G. W., Markert, T. H., and Winkler, P. F. 1980, *Ap. J. (Letters)*, **241**, L151.
 Shull, J. M., Fesen, R. A., and Saken, J. M. 1989, *Ap. J.*, **346**, 860.
 Shull, P., Jr., Carsenty, V., Sarcander, M., and Neckel, T. 1985, in *The Crab and Related Supernova Remnants*, ed. M. C. Kafatos and R. Henry (New York: Cambridge University Press), p. 127.
 Sivan, J. P. 1974, *Astr. Ap. Suppl.*, **16**, 163.
 Trimble, V. 1971, in *IAU Symposium 46, The Crab Nebula*, ed. R. Davis and F. G. Smith (Dordrecht: Reidel), p. 12.
 Velusamy, T. 1985, *M.N.R.A.S.*, **212**, 359.
 Weaver, H., and Williams, D. 1974, *Astr. Ap. Suppl.*, **17**, 1.

CARL HEILES, BON CHUL KOO, and WILLIAM T. REACH: Astronomy Department, University of California, 601 Campbell Hall, Berkeley, CA 94720

ROGER W. ROMANI: Institute for Advanced Study, School of Natural Science, Princeton, NJ 08540